ISPRS Journal of Photogrammetry and Remote Sensing 64 (2009) 674–682

Contents lists available at ScienceDirect

ISPRS Journal of Photogrammetry and Remote Sensing

journal homepage: www.elsevier.com/locate/isprsjprs

Estimation of abundance and distribution of two moist tall grasses in the Watarase wetland, Japan, using hyperspectral imagery

Shan Lu [1], Yo Shimizu, Jun Ishii, Syo Funakoshi, Izumi Washitani, Kenji Omasa *

Graduate School of Agricultural and Life Sciences, The University of Tokyo, 1-1-1 Yayoi, Bunkyo-ku, Tokyo 113-8657, Japan

ARTICLE INFO

Article history:
Received 12 March 2008
Received in revised form
28 May 2009
Accepted 19 June 2009
Available online 6 August 2009

Keywords:
Hyperspectral
Imagery
Estimation
Vegetation

ABSTRACT

The dominant grasses in a wetland are of critical concern for the wetland's ecological integrity, because these species provide the habitats for many small plants and animals. In this study, we used hyperspectral imagery to map the distributions of two dominant tall grasses (*Miscanthus sacchariflorus* (Maxim.) Benth and *Phragmites australis* (Cav.) Trin. ex Stend) in the Watarase wetland, in central Japan. Stepwise multiple linear regression analysis was applied to the hyperspectral data to predict the shoot density and biomass of the two grasses. The independent data sets included original reflectance, band ratios, significant components identified by principal components analysis (PCA), and significant components identified by decision boundary feature extraction (DBFE). The coefficient of determination (R^2) and the root-mean-square error (RMSE) of model calibration and validation were used to evaluate the models. The significant DBFE components showed better ability at predicting shoot density of the two grasses than the other variables in the validating areas. The RMSE values were 7.40/m^2 for *M. sacchariflorus* and 13.09/m^2 for *P. australis*, which amounted to errors of around 10.0% and 12.6%, respectively, of the maximum shoot density measured during our surveys. All variables showed similar performance at predicting biomass, but the results were less accurate than those for shoot density. Considering the performance of the DBFE components for both shoot density and biomass prediction, we suggest that these are the best indicators for estimating the abundance of the two grasses.

1. Introduction

The importance of wetlands functions and their values have been increasingly recognized. Far from being useless, disease-ridden places, wetlands provide values that no other ecosystem can, including improvement of water quality, flood protection, shoreline erosion control, opportunities for recreation and aesthetic appreciation, and the provision of natural products for our use (Toyra et al., 2001). Wetlands are also valued because they provide a unique habitat for a wide variety of plants, fish, wildlife, and invertebrates, including many threatened or endangered species (Chiras, 2006). Thus, monitoring of the vegetation that occupies wetland habitats is very important if we are to learn how to protect these wetlands.

The Watarase wetland is the largest lowland wetland in central Japan. It is dominated by two tall grasses: *Miscanthus sacchariflorus* (Maxim.) Benth and *Phragmites australis* (Cav.) Trin. ex Stend. These two grasses, which have a very similar morphology, are important to the ecological integrity of the wetland because they provide habitats for many small plants and animals (Washitani, 2001). For example, some endangered plant species in the Watarase wetland are associated with specific habitats where one of the dominant grass species predominates or where both are mixed more evenly. Therefore, discriminating between the two grasses may help wetland managers to determine the potential habitat areas for the endangered plant species. Knowledge of the spatial distribution and dynamics of the dominant grasses can be achieved through field monitoring, but access limitations and the requirement for time-consuming surveys may make the cost of such direct monitoring prohibitive.

Researchers have recently considered performing such surveys by taking advantage of remote-sensing techniques, which are expected to overcome the disadvantages of direct surveys. Remotely sensed imagery has frequently been used in wetland mapping (Ackleson and Klemas, 1987; Jensen et al., 1984). However, these studies have mainly concerned the use of multispectral imagery, and few have adopted hyperspectral remote sensing techniques (Hirano et al., 2003). Unfortunately, wetland vegetation can be confused with different land cover classes when

* Corresponding author. Tel.: +81 3 5841 5340; fax: +81 3 5841 8175.
E-mail address: aomasa@mail.ecc.u-tokyo.ac.jp (K. Omasa).
[1] Present address: College of Urban and Environmental Sciences, Northeast Normal University, 5268 Renmin Street, Changchun 130024, China.

0924-2716/$ – see front matter
doi:10.1016/j.isprsjprs.2009.06.003

multispectral imagery is used because of the problem of overlapping spectral signatures (Ozesmi and Bauer, 2002). At the level of species differentiation, such as differentiation of the two very similar dominant grasses in the Watarase wetland, mapping of vegetation properties requires the detection of subtle differences in canopy density, leaf and canopy structure, and biochemical properties. Therefore, imaging spectrometers (hyperspectral sensors) are particularly well-suited for this task because of the type and amount of spectral information they collect (Rosso et al., 2005).

Some hyperspectral data-analysis algorithms have been developed and applied to vegetation discrimination and biochemistry estimation. For example, unmixing of the hyperspectral data is a good means to estimate the distribution of vegetation (Dehaan et al., 2007). Adams et al. (1986) used spectral-mixture analysis to discriminate species at the sub-pixel level, and found that it was possible to determine the relative percentages of various classes in a single pixel. Previously, we tried to estimate the abundance of the two dominant tall grasses in the Watarase wetland by using a partial-unmixing, matched-filtering method, but it was difficult to obtain pure pixels as targets for each grass, which is a necessary step in the matched-filtering process. We found that the selection of *P. australis* endmembers was harder than that of *M. sacchariflorus* endmember (Lu et al., 2006).

Some researchers have shown that statistical methods can be used to effectively process hyperspectral data without the limitations imposed by the unmixing procedure. For example, Galvão et al. (2005) applied multiple-discriminant analysis to surface reflectance values, reflectance ratios, and several spectral indices, and were able to discriminate five important Brazilian sugarcane cultivars. Kokaly and Clark (1999) developed a method for estimating the biochemical properties of plant material using hyperspectral spectroscopy. They used stepwise multiple linear regression to select wavelengths from the overall absorption features that were most strongly correlated with the chemistry of the samples. By applying the derived linear equations to the validation data, the authors were able to successfully estimate the nitrogen, lignin, and cellulose concentrations in different plant species. These studies have focused on the discrimination of plant species or their biochemical characteristics, but have seldom been used to obtain biophysical information such as shoot density or biomass of wetland vegetation.

In the present study, our goal was to propose a feasible method for estimating the abundance and distribution of *M. sacchariflorus* and *P. australis* in the Watarase wetland using stepwise regression models to analyze data obtained by hyperspectral imagery. We chose four sets of independent variables for use in the stepwise regression analysis to predict plant shoot density and biomass: the original reflectance values, the band ratios, the components of principal components analysis (PCA), and decision boundary feature extraction (DBFE). The selection of key original reflectance values and band ratios has been successfully used to estimate the chlorophyll concentration of plants (Chappelle et al., 1992), to classify vegetation (Galvão et al., 2005), and to map the distribution of white micas (van Ruitenbeek et al., 2006). PCA (Jia and Richards, 1999) and DBFE (Lee and Landgrebe, 1993) have also been commonly used to extract the spectral features from imaging data and to reduce the number of data dimensions required for classification of image pixels. Here, we tested the ability of all four approaches to identify the best set of independent variables for mapping the abundance of the two grasses in the Watarase wetland.

2. Materials and methods

2.1. Study area

The Watarase wetland is the largest lowland wetland in central Japan (Fig. 1). The wetland was formed between 1910 and 1926 by damming three rivers to control flooding of downstream areas with contaminated water from a copper mine along the upper reaches of the rivers. Precipitation at the Koga meteorological station, near the Watarase wetland, averaged 1197 mm annually from 1977 to 2004. The study area has a relatively hot-wet summer and cold-dry winter because it is located in an inland part of Japan. More than 650 species of wetland plants grow in the wetland (Ohwada and Ogura, 1996), of which 59 are endangered species that are listed in the national Red List (Ministry of the Environment of Japan, 2007).

M. sacchariflorus and *P. australis* start growing in March of each year after the wetland undergoes controlled burning by its managers. After the burning, both grasses reach their maximum height (around 4 m) in July and August. During the growth period, *P. australis* develops faster than *M. sacchariflorus*. The largest difference in plant form between the species occurs at the end of May. This difference in the phenology of the grasses makes the end of May a good time to capture hyperspectral imagery and use it to differentiate between them. The grasses flower from September to October and bear seeds in November and December.

2.2. AISA Eagle imagery

The images used in this study were acquired by the Eagle Airborne Imaging Spectroradiometer for Application (AISA) hyperspectral system. The AISA consists of a compact hyperspectral sensor head, a miniature GPS/INS sensor, a data-acquisition computer, the RSCube software, and a power supply. The instrument collected images at nadir in 68 contiguous spectral bands, sampled at approximately 9-nm intervals in the range from 398 to 984 nm. The nominal flight altitude is around 1400 m above the ground, resulting in a pixel size of 1.5 × 1.5-m. The sensor was flown over the eastern part of the Watarase wetland (see Fig. 1). Radiance was calculated as the upwelling radiant energy received at the sensor, and the apparent reflectance was defined as the ratio between upwelling and downwelling radiant energy. The downwelling radiant energy from the sun was measured by the onboard fiber optic downwelling irradiance sensor (FODIS). Images were recorded as the apparent reflectance measured at the instrument height.

The flight over the Watarase wetland was carried out on 26 May 2005, when the two dominant grasses were showing their peak differences in plant form. In this study, we used two mosaic-processed strips of images in areas where the dominant grasses were most abundantly distributed. Each strip of data had a nominal cross-track swath width of about 1 km and a down-track image length of about 6 km. Because the two strips overlapped in some areas, the total area covered was about 8 km^2. The areas outside the moist grassland were subtracted before the analysis.

2.3. Field data acquisition

Detailed field information on the dominant grasses was obtained from the end of May to the middle of June 2005. Thirty-eight 5 × 5-m plots were established to determine the abundance of *M. sacchariflorus* and *P. australis*. In each plot, three 1 × 1-m subplots were randomly chosen to measure different parameters. The means from the three subplots were used to represent each 5 × 5-m plot. The locations of the four corners of each plot were recorded on a Trimble Pathfinder ProXR GPS device. The four corner points were then plotted on the georeferenced AISA images. The estimated positional error was less than 1 pixel.

We measured shoot densities by counting all shoots in each of the three subplots and shoot heights by measuring all the shoots counted in each plot. The shoot heights were used to estimate the aboveground biomass. Because the shoot heights were incorrectly measured in three plots during the fieldwork, we had only 35

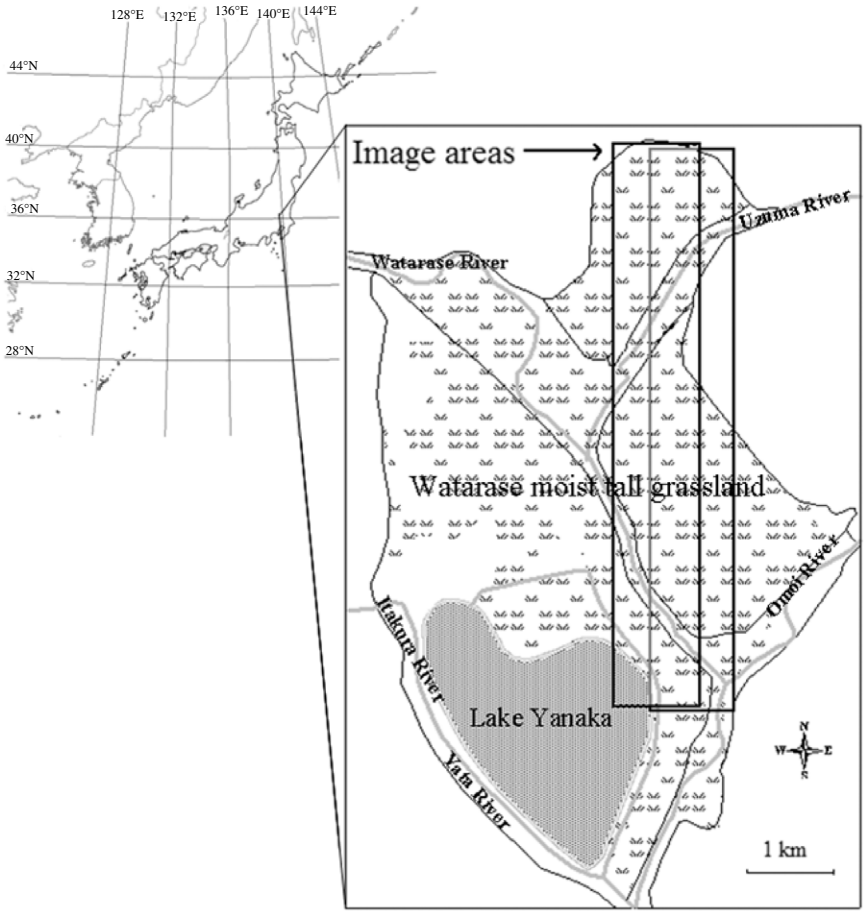

Fig. 1. Location of the study area.

samples available for calculating biomass. After measuring the shoot height, we cut 50 shoots at the roots from each grass species. The shoots were then brought to the laboratory to measure the individual aboveground dry weight after oven-drying for 3 days at 80 °C.

The regression equations used to calculate the biomass are shown as Eq. (1) for *M. sacchariflorus* and Eq. (2) for *P. australis*:

Dry weight (*M. sacchariflorus*)

$$= 0.0005h^2 - 0.0024h - 2.0437 \ (R^2 = 0.85) \quad (1)$$

Dry weight (*P. australis*)

$$= 0.0007h^2 - 0.1021h + 7.1806 \ (R^2 = 0.93) \quad (2)$$

where h indicates the mean shoot height (cm) of the plants in a plot for a given species. We calculated the dry weight per shoot in each plot by using the average shoot height in the regression equation. This weight was multiplied by number of plants in 1 m^2 to obtain the biomass per unit area (g/m^2).

2.4. Relating plant abundance to spectral reflectance and transformed reflectance

We randomly selected half of the samples (the training samples) from the field survey plots, and used them to develop a regression model for the estimation of plant abundance, and used the other half (the validation samples) to validate the models. The mean and variance of the two data sets were not significantly different, which made it possible to evaluate the predictive performance of the models. The number of training samples used in constructing the shoot density and biomass models was 19 and 17, respectively.

We used stepwise multiple linear regression to predict the shoot density and biomass as a function of the reflectance value or other transformed reflectance parameters. We used the F-test to include ($P < 0.05$) and to remove ($P \geq 0.1$) variables in the forward and backward steps. We chose four sets of independent variables for this analysis. The first set comprises the original reflectance data, but the other three were parameters sets created by transforming that data. The first transformed set represented the ratios between the hyperspectral band data. We calculated all the ratios between each pair of bands, and obtained 4556 ($68 \times 68 - 68$) ratios for the 68 bands. The total number was too large to analyze statistically, since the number of dependent variables was fewer than 20 in this analysis. Instead, we first calculated the coefficients of correlation between the band ratios and plant abundance, then selected the 200 ratios with the largest correlation coefficients as the independent variables. The second transformed set comprised the components of the PCA. PCA relies on the fact that most of the variance in the image can be represented by the first few components. We selected up to six components for which the cumulative variance was greater than 99% as the independent variables. The third set comprised the components of the DBFE. DBFE extracts the features that can be used most effectively to classify image pixels into categories. We selected up to 18 DBFE components for which the cumulative variance was greater than 99% as the independent variables. We used the PCA and DBFE feature-extraction methods to qualitatively classify the species of the two similar tall grasses and to quantitatively estimate their shoot density and biomass.

Table 1
Statistical description of the two grass species in the Watarase wetland.

		Mean	Maximum	Std. deviation
Miscanthus sacchariflorus	Shoot density ($/m^2$) ($N = 38$)	20.52	74.30	22.61
	Biomass (g/m^2) ($N = 35$)	219.32	1204.02	321.70
Phragmites australis	Shoot density ($/m^2$) ($N = 38$)	24.18	103.70	24.39
	Biomass (g/m^2) ($N = 35$)	267.55	1219.39	326.48

Among the four sets of variables, the original reflectance, band ratios, and PCA have been commonly used in many remote-sensing data analysis studies (Byrne et al., 1980; De Jong et al., 2003; Doxaran et al., 2002). DBFE, however, was originally a feature-extraction method proposed for use in classification by Lee and Landgrebe (1993). The theory behind DBFE requires the computation of the decision boundaries among the classes by means of a training set. It can be demonstrated that the rank of the so-called decision boundary characteristic matrix is also the minimum data dimension required to obtain the same classification results as with the original hyperspectral data in the training data set. Correspondingly, the eigenvectors with non-null eigenvalues extracted from the same matrix represent the directions of projections of the original data that satisfy the aforementioned condition. The DBFE method has been proved to be very effective in classifying similar crops in agricultural land (Lu et al., 2007). To process the DBFE, a pure training set for each grass is necessary. We selected the plots with the largest shoot density as the training area for each grass.

3. Results and discussion

3.1. Measured shoot density and biomass

Table 1 summarizes the statistical characteristics of the shoot density and biomass of each species based on the field survey. *P. australis* grew more densely than *M. sacchariflorus*. However, the plot with the maximum biomass did not necessarily correspond to the plot with the maximum shoot density, because the biomass reported here is an estimate based on the shoot height. The similar maximum biomasses of both grasses suggest the existence of a productivity limit in the Watarase wetland, regardless of the vegetation species.

3.2. Spectral reflectance and transformed reflectance parameters selected by stepwise multiple linear regression

Table 2 shows the wavelengths or components that were selected to formulate the regression models for shoot density and biomass by means of stepwise multiple linear regression. Four wavelengths were selected in the regression model of *M. sacchariflorus* shoot density using the original reflectance values. Two of the four wavelengths selected were near 550 nm, which is related to the vegetation's green color, and one was near red range of 700 nm. On the other hand, only two wavelengths were required to estimate the shoot density of *P. australis*, one in the green range (524 nm) and the other in the red range (684 nm). Three wavelengths were selected in the regression model for *M. sacchariflorus* biomass using the original reflectance values. Two of these were near the visible wavelengths of the green band, and the third was at the edge of the visible spectrum (719 nm). In the *P. australis* biomass estimation, a single wavelength (920 nm, in the near-infrared) was selected.

In the regression model that used the band ratios as independent variables, only one ratio (630 nm/692 nm) was selected to estimate the shoot density of *M. sacchariflorus*. In contrast, four band ratios (692 nm/559 nm, 621 nm/541 nm, 639 nm/559 nm, and 603 nm/550 nm) were required in the regression model for estimating the shoot density of *P. australis*. Most of the wavelengths used for the four ratios are concentrated in the green and red bands. For the biomass of *M. sacchariflorus*, two ratios (550 nm/710 nm and 710 nm/533 nm) were selected, suggesting that ratios that incorporated the 710-nm wavelength were sensitive to the biomass of *M. sacchariflorus*. For the biomass of *P. australis*, only one ratio (737 nm/550 nm) was selected.

Among the first six components of the PCA, the first, third, fifth, and sixth were significant in estimating the shoot density and biomass of the two species. The sixth component was selected for estimating the shoot density of both species. This suggests that the sixth component is a significant index of their distribution and abundance. The third component was also selected as an important factor in the regression models to estimate the abundance of *M. sacchariflorus*. Only the sixth component was selected for shoot density of *P. australis*, and only the first component was selected for biomass.

Among the 18 components of the DBFE, three were required in every regression model to estimate the shoot density and biomass of the two grasses. The second and eleventh components were selected for the regression models for both shoot density and biomass of *M. sacchariflorus*. For *P. australis*, different components were selected for the two regression models.

It should be noted that it is difficult to conceptually relate each PCA or DBFE component to areas with a specific characteristic, because the hyperspectral imagery was transformed to create the feature space. Therefore, the variables induced from the reflectance transformation in the PCA and DBFE analyses have the disadvantage of being unintuitive and difficult to interpret.

3.3. Estimating plants abundance in the training samples

Table 3 shows the adjusted R^2 and the root-mean-square error (RMSE) values for the shoot density and biomass of each species estimated from each set of independent variables, and the ratio of RMSE to the maximum value of each parameter determined in the field survey. With a few exceptions, the correlations obtained by means of DBFE were generally higher, and the RMSE values were generally lower. Figs. 2 and 3 show the scatter plots of the relationship between the regression estimates based on the DBFE components for the shoot density and biomass of both species.

Table 2
Reflectance values and transformed reflectance values correlated with the abundance of the two species that were selected using stepwise linear regression from the training samples. (For PCA and DBFE, "C" represents the component number.)

		Original reflectance	Band ratio	Principal components analysis (PCA)	Decision boundary feature extraction (DBFE)
Miscanthus sacchariflorus	Shoot density	701, 568, 533, and 447 nm	630 nm/692 nm	C6, C3, C5	C2, C9, C11
	Biomass	719, 541, and 585 nm	550 nm/710 nm, 710 nm/533 nm	C3, C6	C3, C11, C2
Phragmites australis	Shoot density	684 and 524 nm	692 nm/559 nm, 621 nm/541 nm, 639 nm/559 nm, 603 nm/550 nm	C6	C1, C4, C15
	Biomass	920 nm	737 nm/550 nm	C1	C14, C18, C2

Table 3
Results of using stepwise multiple linear regression to estimate plant abundance from the training samples. (The values in brackets represent the ratios of the root-mean-square error (RMSE) to the corresponding maximum shoot density or biomass from the field survey.)

		Original reflectance		Band ratio		Principal components analysis (PCA)		Decision boundary feature extraction (DBFE)	
		R^2	RMSE	R^2	RMSE	R^2	RMSE	R^2	RMSE
Miscanthus sacchariflorus	Shoot density (/m^2) ($N = 19$)	0.97	3.74 [5.0%]	0.83	9.13 [12.3%]	0.81	9.21 [12.4%]	0.90	6.84 [9.2%]
	Biomass (g/m^2) ($N = 17$)	0.83	80.56 [6.7%]	0.96	39.23 [3.3%]	0.83	79.89 [6.6%]	0.86	75.06 [6.2%]
Phragmites australis	Shoot density (/m^2) ($N = 19$)	0.59	15.56 [15.0%]	0.95	13.41 [12.9%]	0.43	18.38 [17.7%]	0.81	9.85 [9.5%]
	Biomass (g/m^2) ($N = 17$)	0.64	186.62 [15.3%]	0.69	165.46 [13.6%]	0.63	188.16 [15.4%]	0.70	150.46 [12.3%]

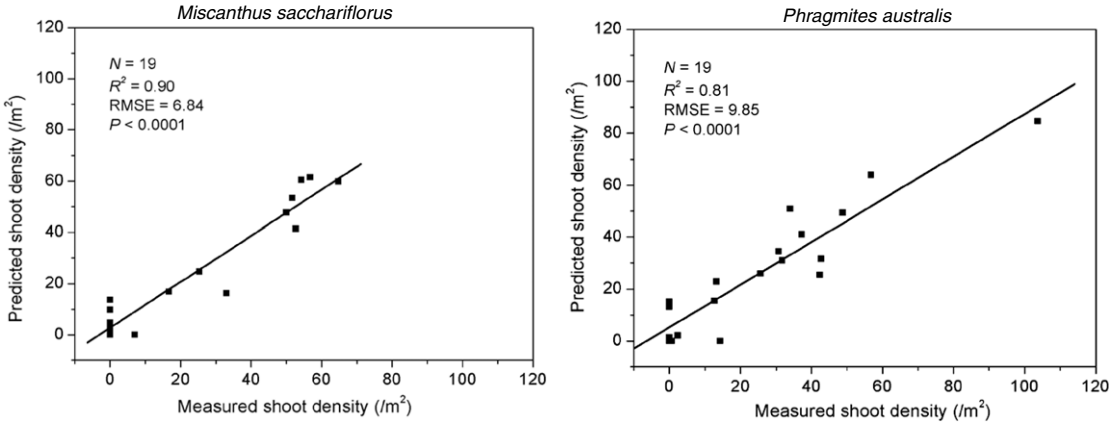

Fig. 2. Relationships between estimated and measured shoot density (using the training samples and the DBFE components) for *Miscanthus sacchariflorus* and *Phragmites australis*.

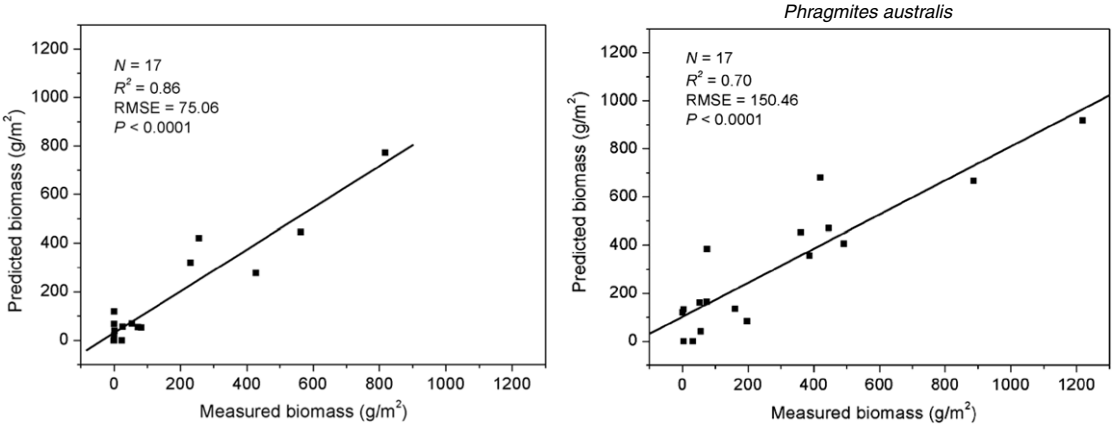

Fig. 3. Relationships between estimated and measured biomass (using the training samples and the DBFE components) for *Miscanthus sacchariflorus* and *Phragmites australis*.

The patterns of shoot density estimates differed between the species. For *M. sacchariflorus*, the original reflectance values produced the highest correlation coefficient (adjusted $R^2 = 0.97$) and the lowest RMSE (3.74/m^2, representing a 5.0% error compared with the maximum shoot density in the field survey). The band ratio method had the highest correlation coefficient (adjusted $R^2 = 0.95$) for estimating the shoot density of *P. australis*, but the RMSE was high (13.41/m^2, representing a 12.9% error), because one point was estimated particularly poorly. The lowest RMSE for *P. australis* shoot density (9.85/m^2, representing a 9.5% error) was obtained from the DBFE components.

Similarly, the biomass estimates differed between the species. The best method for estimating the biomass of *M. sacchariflorus* was the band ratio method. It had the highest adjusted R^2 (0.96), and an RMSE of 39.23 g/m^2 (3.3% of the maximum biomass in the field survey). For *P. australis*, the best method was the DBFE approach, with an adjusted R^2 of 0.70 and an RMSE of 150.46 g/m^2 (12.3% error).

The results demonstrate that no one approach produced the smallest RMSE for both biophysical parameters or both species. However, it is important to note that choosing the best set of variables should not be based on validation using the training samples that were used to construct the regression models. A more convincing validation would be provided by using different validation samples that were not used to construct the regression models. Therefore, we repeated our validation of the regression models using the validation samples.

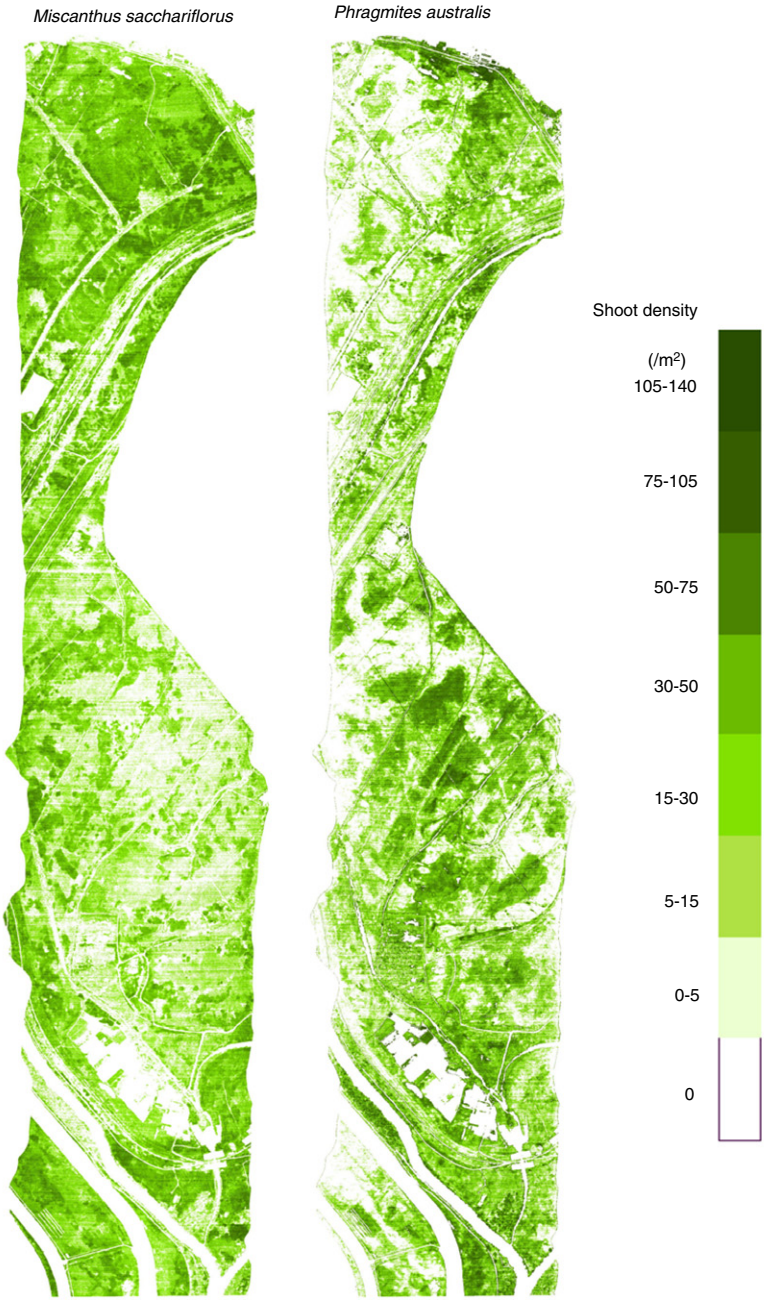

Fig. 4. Distribution of shoot density of *Miscanthus sacchariflorus* and *Phragmites australis*.

Table 4
Root-mean-square errors (RMSE) of the stepwise multiple linear regression equations used to predict the validation samples. (The values in brackets represent the ratios of the RMSE to the corresponding maximum shoot density or biomass from the field survey.)

		Original reflectance	Band ratio	Principal components analysis (PCA)	Decision boundary feature extraction (DBFE)
Miscanthus sacchariflorus	Shoot density ($/m^2$) ($N = 19$)	21.84 [29.4%]	13.32 [17.9%]	16.77 [22.6%]	7.40 [10.0%]
	Biomass (g/m^2) ($N = 18$)	196.46 [16.3%]	137.33 [11.4%]	158.97 [13.2%]	143.70 [11.9%]
Phragmites australis	Shoot density ($/m^2$) ($N = 19$)	18.88 [18.2%]	18.06 [17.4%]	15.04 [14.5%]	13.09 [12.6%]
	Biomass (g/m^2) ($N = 18$)	200.94 [16.5%]	222.25 [18.2%]	200.90 [16.5%]	204.80 [16.8%]

3.4. Evaluating the predictive ability of regression models

We re-evaluated the predictive ability of the models using the validation data from the survey plots (19 samples for shoot density and 18 for biomass). Table 4 presents the resulting RMSE values and the corresponding error percentages as a function of the maximum values from the field survey.

The RMSE values for the validation samples were generally higher than those for the training samples. In predicting the plant shoot density, the DBFE components showed the best predictive ability for both grasses. The RMSE for *M. sacchariflorus* was 7.40 $/m^2$, which represents a 10.0% error relative to the maximum surveyed shoot density. The RMSE for *P. australis* was 13.09 $/m^2$, which represents a 12.6% error. Interestingly, the RMSE values

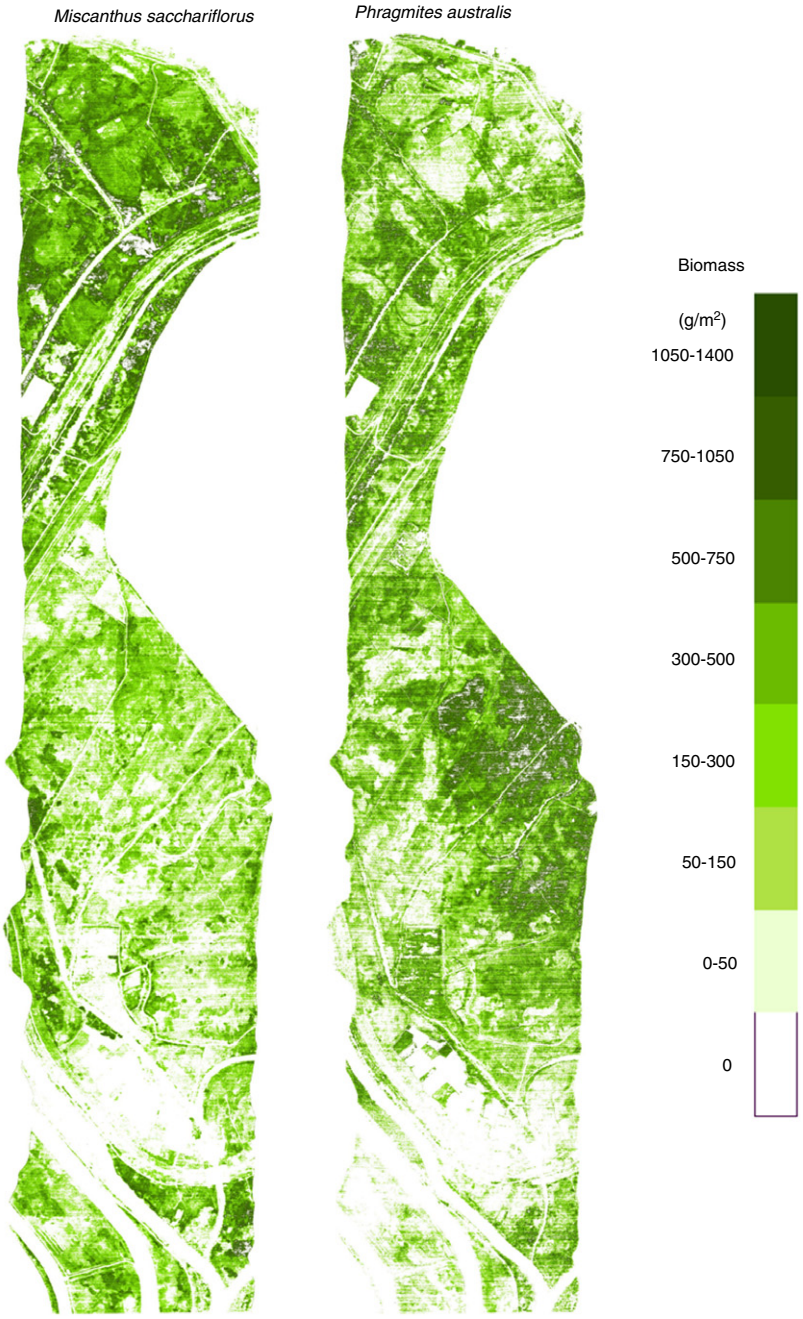

Fig. 5. Distribution of biomass of *Miscanthus sacchariflorus* and *Phragmites australis*.

for the regression models derived from the DBFE components for the training samples (Table 3) increased less for the validation samples (Table 4) than those for the models derived from the other three variable sets. The good predictive ability using the DBFE components suggests that these components may provide the most accurate estimates of the shoot density of the two species in the Watarase wetland. This good performance results from the fact that the DBFE components were extracted from hyperspectral data which specially distinguish the two species. It is encouraging that the information included in the DBFE components also enabled quantitative estimation of vegetation biophysical parameters, not only a qualitative classification discussed in the past studies (Benediktsson and Sveinsson, 1997; Lu et al., 2007)

In predicting the biomass of the two species, the models derived from the four sets of variables showed similar results. For *M. sacchariflorus*, the RMSE ranged from 137.33 to 196.46 g/m^2, and the corresponding percentages of the maximum biomass in the field surveys ranged from 11.4% to 16.3%. On the other hand, the RMSE for *P. australis* ranged from 200.90 to 222.25 g/m^2, with corresponding percentages of 16.5% to 18.2%. For biomass estimation, the DBFE approach generally produced results at least as good as those obtained using the other sets of variables. Considering that the DBFE components performed better than the other methods for estimating shoot density and equally good results for biomass prediction, we selected them as the best indicators to estimate the abundance of both grasses.

The errors as a proportion of the maximum biomass were larger than the errors as a proportion of maximum shoot density, thus the hyperspectral imagery appears to be more effective for estimating shoot density than biomass in the study area.

Figs. 4 and 5 show the distributions of the shoot density and biomass of the two grasses predicted using the DBFE components.

Fig. 6. The relative dominance of the two grasses based on their respective shoot densities.

Either *M. sacchariflorus* or *P. australis* occupied most of the study area. Fig. 6 shows the relative dominance derived from the shoot density map for the two species. The dominance values were calculated by dividing the total shoot density in each pixel by the corresponding *M. sacchariflorus* shoot density. The northwestern area was dominated by *M. sacchariflorus*, and the southern area by *P. australis*. The two grasses were relatively evenly distributed in the northeast. The ability of the DBFE approach to distinguish between the two species suggests that this method has considerable potential for revealing the distribution of endangered species that are associated with the two study species.

4. Conclusions

This paper describes a methodology for estimating the abundance and distribution of two morphologically similar species, *M. sacchariflorus* and *P. australis*, in the Watarase wetland by identifying the most useful variables among several sets of independent variables derived from hyperspectral reflectance data, and by correlating them with shoot density and biomass by means of stepwise multiple linear regression. The original reflectance and the transformed reflectance parameters based on band ratios, PCA, and DBFE were used as the independent variables. The results suggest

that the regression based on the DBFE components had the best ability at estimating the shoot density of both species, and predictive ability comparable to that of the other methods for estimating the biomass of both species. The models based on the DBFE components performed well because the DBFE components included information that specifically distinguished between the two similar grasses. However, further study will be needed to interpret the physical meaning of the components selected by the DBFE analysis.

The results also suggest the possibility of developing generally applicable models that could be used to simply and rapidly estimate and map the abundance and distribution of these grasses in the Watarase wetland on the basis of hyperspectral imagery, thereby facilitating studies of the wetland's ecological integrity.

Acknowledgements

We thank two anonymous reviewers for their valuable comments on earlier versions of this manuscript.

References

Ackleson, S.G., Klemas, V., 1987. Remote sensing of submerged aquatic vegetation in Lower Chesapeake Bay: A comparison of Landsat MSS to TM imagery. Remote Sensing of Environment 22 (2), 235–248.

Adams, J.B., Smith, M.O., Johnson, P.E., 1986. Spectral mixture modeling: A new analysis of rock and soil types at the Viking Lander 1 site. Journal of Geophysical Research 91 (B8), 8098–8112.

Benediktsson, J.A., Sveinsson, J.R., 1997. Feature extraction for multisource data classification with artificial neural networks. International Journal of Remote Sensing 18 (4), 727–740.

Byrne, G.F., Crapper, P.F., Mayo, K.K., 1980. Monitoring land-cover change by principal component analysis of multitemporal Landsat data. Remote Sensing of Environment 10 (3), 175–184.

Chappelle, E.W., Kim, M.S., McMurtrey, J.E., 1992. Ratio analysis of reflectance spectra (RARS): An algorithm for the remote estimation of the concentrations of chlorophyll a, chlorophyll b, and carotenoids in soybean leaves. Remote Sensing of Environment 39 (3), 239–247.

Chiras, D.D., 2006. Environmental Science, seventh ed. Jones and Bartlett Publishers, Sudbury.

Dehaan, R., Louis, J., Wilson, A., Hall, A., Rumbachs, R., 2007. Discrimination of blackberry (*Rubus fruticosus* sp. agg.) using hyperspectral imagery in Kosciuszko National Park, NSW, Australia. ISPRS Journal of Photogrammetry and Remote Sensing 62 (1), 13–24.

De Jong, S.M., Pebesma, E.J., Lacaze, B., 2003. Above-ground biomass assessment of Mediterranean forests using airborne imaging spectrometry: The DAIS Peyne experiment. International Journal of Remote Sensing 24 (7), 1505–1520.

Doxaran, D., Froidefond, J.-M., Castaing, P., 2002. A reflectance band ratio used to estimate suspended matter concentrations in sediment-dominated coastal waters. International Journal of Remote Sensing 23 (23), 5079–5085.

Galvão, L.S., Formaggio, A.R., Tisot, D.A., 2005. Discrimination of sugarcane varieties in Southeastern Brazil with EO-1 Hyperion data. Remote Sensing of Environment 94 (4), 523–534.

Hirano, A., Madden, M., Welch, R., 2003. Hyperspectral image data for mapping wetland vegetation. Wetlands 23 (2), 436–448.

Jensen, J.R., Christensen, E.J., Sharitz, R., 1984. Nontidal wetland mapping in South Carolina using airborne multispectral scanner data. Remote Sensing of Environment 16 (1), 1–12.

Jia, X., Richards, J.A., 1999. Segmented principal components transformation for efficient hyperspectral remote sensing image display and classification. IEEE Transactions on Geoscience and Remote Sensing 37 (1), 538–542.

Kokaly, R.F., Clark, R.N., 1999. Spectroscopic determination of leaf biochemistry using band-depth analysis of absorption features and stepwise multiple linear regression. Remote Sensing of Environment 67 (3), 267–287.

Lee, C., Landgrebe, D.A., 1993. Feature extraction based on decision boundaries. IEEE Transactions on Machine Intelligence 15 (4), 388–400.

Lu, S., Funakoshi, S., Shimizu, Y., Ishii, J., De Asis, A.M., Washitani, I., Omasa, K., 2006. Estimation of plant abundance and distribution of *Miscanthus sacchariflorus* and *Phragmites australis* using matched filtering of hyperspectral image. Eco-Engineering 18 (2), 65–70.

Lu, S., Oki, K., Shimizu, Y., Omasa, K., 2007. Comparison between several feature extraction/classification methods for mapping complicated agricultural land use patches using airborne hyperspectral data. International Journal of Remote Sensing 28 (5), 963–984.

Ministry of the Environment of Japan, 2007. Red list of vascular plants (in Japanese). http://www.env.go.jp/press/file_view.php?serial=10251&hou_id=8886 (accessed on 23.06.09).

Ohwada, M., Ogura, H., 1996. A floristic study of Watarase retarding basin. Bulletin of the Tochigi Prefectural Museum 13, 31–108 (in Japanese with English abstract).

Ozesmi, S.L., Bauer, M.E., 2002. Satellite remote sensing of wetlands. Wetlands Ecology and Management 10 (5), 381–402.

Rosso, P.H., Ustin, S.L., Hastings, A., 2005. Mapping marshland vegetation of San Francisco Bay, California, using hyperspectral data. International Journal of Remote Sensing 26 (23), 5169–5191.

Toyra, J., Pietroniro, A., Martz, L.W., 2001. Multisensor hydrologic assessment of a freshwater wetland. Remote Sensing of Environment 75 (2), 162–173.

van Ruitenbeek, F.J.A., Debba, P., van der Meer, F.D., Cudahy, T., van der Meijde, M., Hale, M., 2006. Mapping white micas and their absorption wavelengths using hyperspectral band ratios. Remote Sensing of Environment 102 (3–4), 211–222.

Washitani, I., 2001. Plant conservation ecology for management and restoration of riparian habitats of lowland Japan. Population Ecology 43 (3), 189–195.